IJE TRANSACTIONS C: Aspects Vol. 29, No. 06, (June 2016) 834-842

International Journal of Engineering

Journal Homepage: www.ije.ir

Nonlinear Dynamics of the Rotational Slender Axially Moving String with Simply Supported Conditions

H. Heydari[a], M.R. Ghazavi*[a], A. Najafi[b], S. Rahmanian[a]

[a] *Department of Mechanical Engineering, Tarbiat Modares University, Tehran, Iran*
[b] *Mechanical Rotary Equipment Department, Niroo Research Institute, Tehran, Iran*

PAPER INFO

Paper history:
Received 16 December 2015
Received in revised form 07 April 2016
Accepted 02 June 2016

Keywords:
String
Axial Speed
Bifurcation Diagram
Poincare Portrait
Quasi-periodic

ABSTRACT

In this research, dynamic analysis of the rotational slender axially moving string is investigated. String is assumed as Euler Bernoulli beam. The axial motion of the string, gyroscopic force and mass eccentricity were considered in the study. Equations of motion are derived using Hamilton's principle, resulting in two partial differential equations for the transverse motions. The equations are changed to non-dimensional form and are discretized via Galerkin' method. The bifurcation diagrams and Poincare' portraits are represented in the case that the mean axial speed, the fluctuating speed and the mass eccentricity are respectively varied. The dynamical behaviors are numerically identified based on the Poincare' portraits. Numerical simulations indicate that quasi-periodic motion occurs in the transverse vibrations of the string by variation of axial speed and mass eccentricity.

***doi**: 10.5829/idosi.ije.2016.29.06c.13*

NOMENCLATURE

D_i	Inside diameter of the string, m
D_o	Outside diameter of the string , m
A_p	Cross sectional area of the string , m^2
E	Young's modulus of the string, Pa
e_0	Mass eccentricity of the string, m
I	Area moment of inertia, m^4
I_0	Polar area moment of inertia, m^4
l	Length of the string, m
v, w	Lateral deflections, m
ρ_p	String material density, kg/m^3
μ_p	Axial speed of the string , m/s
Ω	String rotational speed, rad/s
C_v, C_w	Lateral damping coefficients

*Corresponding Author's Email: *ghazavim@modares.ac.ir* (D. Ghazavi)

Please cite this article as: H. Heydari, M.R. Ghazavi, A. Najafi, S. Rahmanian, Nonlinear Dynamics of the Rotational Slender Axially Moving String with Simply Supported Conditions, International Journal of Engineering (IJE), TRANSACTIONS C: Aspects Vol. 29, No. 06, (June 2016)

1. INTRODUCTION

Dynamic analysis of axially moving systems especially one-dimensional systems (beams and strings), has been subjected of investigations for many years because of their extensive applications. For instance, drill string (for drilling of the wells in oil and gas industries) band saw blades, robotic manipulator, conveyor belts, textile fibers, automobile and aerospace structures can be modeled as axially moving systems. Mentioned engineering devices involve the vibrations of axially moving beams. Traditionally, the investigations on axially moving beams were concentrated on equilibriums and periodic motions [1]. Bifurcation is a qualitative change in the feature of the system, such as the number and type of solutions, under the variation of one or more of its control parameter on which the considered system depends [2]. Argyris et al. [3] investigated chaotic vibrations of a nonlinear viscoelastic beam. In recent years, much attention has been paid to nonlinear dynamical behaviors, especially bifurcation and chaos in axially accelerating beams. Pakdemirli and Ulsoy [4] investigated the dynamic response of an axially accelerating string. In their study, principal parametric resonances and combination resonances are investigated in detail. It is found that instabilities occur when the frequency of velocity fluctuations is close to two times that of system natural frequency or when the frequency is close to the sum of any two natural frequencies.

Oz et al. [5] investigated nonlinear vibrations of an axially moving beam. In this study, approximate solutions were sought using method of multiple scales. Results indicated that for frequencies close to two times of the natural frequency, stability and bifurcations of steady state solutions are analyzed. For frequencies close to zero, it is shown that the amplitudes are bounded in time. Chen et al. [6] investigated bifurcation and chaos of an axially moving viscoelastic string. Yang and Chen [7] studied bifurcation and chaos of an axially accelerating viscoelastic beam. They indicated that the periodic, quasi-periodic and chaotic motions occur in the transverse vibrations of the axially accelerating viscoelastic beam with the mean axial speed, speed fluctuation amplitude and the dynamic viscoelasticity as control parameter. Yang et al. [8] investigated non-linear forced vibration of axially moving viscoelastic beams.

In their study, the steady-state amplitude near and exact resonant response is predicted for forced vibrations of viscoelastic moving beams excited by foundation vibration. Results showed that the system vibration amplitude increases with the foundation vibration amplitude and the viscoelastic damping reduces the response amplitude. Sadeghi [9] investigated nonlinear dynamics of a vertical slender flexible cylinder supported at both ends and subjected to axial flow.

Nonlinear Euler Bernoulli beam theory is used for the structure and, the fluid forces acting on the cylinder are assumed to be inviscid, frictional and hydrostatic ones. Finite difference method and AUTO are used as two numerical methods to solve the resulting set of ordinary differential equations. The results for a cylinder with various boundary conditions are presented in the form of bifurcation diagrams with flow velocity as the independent variable, supported by time histories, phase plane plots, PSD plots and Poincaré maps. Wang et al. [10] studied stability and local bifurcation in a simply supported beam carrying a moving mass. They analyzed stability and local bifurcation for 1/2 sub harmonic resonance.

The results showed that some of the parameters, especially the moving mass velocity and external excitation, affect the local bifurcation significantly. Korayem et al. [11] investigated dynamic of moving cable with variable tension and variable speed. Tension force and the moving speed are assumed to be harmonic. Dynamic responses of the system calculated using Galerkin's method. A comprehensive parametric study is carried out and effects of different parameters like the moving speed and tension force on the responses are studied both in frequency and time domain. Ding et al. [12] investigated nonlinear models of transverse vibration of axially moving viscoelastic beams subjected external transverse loads via steady state periodical response. They used finite difference scheme to calculate steady state response for the model of coupled planar and the two models of transverse motion under the simple support boundary. Numerical results indicated that the amplitude of the steady state response for the model of coupled vibration and two models of transverse vibration predict qualitatively the same tendencies with the changing parameters and the integro partial differential equation gives results more closely to the coupled planar vibration. Ghayesh et al. [13] with considering both longitudinal and transverse displacements investigated the nonlinear global forced dynamics of an axially moving viscoelastic beam.

Hosseini et al. [14] studied free vibration and primary resonances of a spinning beam with six general boundary conditions. They employed the method of multiple scales to analyze the free vibrations and primary resonances and then presented Numerical examples for hinged-hinged and clamped-free boundary conditions. Shahgholi et al. [15] studied the free vibration of a nonlinear slender rotating shaft with simply support conditions. The nonlinear system was analyzed utilizing multiple scales method. In the slender rotating shaft the effect of shear deformation was negligible and rotary inertia and gyroscopic effect were considered. It was seen that for natural vibration of a

slender rotating shaft, backward and forward modes were involved. Sahoo et al. [16] analyzed stability and bifurcation of an axially accelerating beam using multiple scales method.

In the aforementioned researches on transverse motions of parametrically excited moving strings, the strings undergo periodic vibrations. Most of these studies devoted to the problem of axial transport velocity. In some studies, the analysis of the dynamic behavior of traveling systems with time dependent axial velocity or with rotation has been addressed. However, time-dependent axial velocity and rotation have been considered simultaneously in this study. Drill string in drilling oil well in oil and gas industry is one of application that time dependent velocity and rotation of the string was considered simultaneously [17-20].

In this research, dynamics of an axially moving beam, subjected to a rotational speed, is examined numerically considering mass eccentricity. The equations of motion are obtained by means of Hamilton' principle. These equations are then discretized using the Galerkin scheme leading to second order ordinary differential equations and they are changed to non-dimensional form by defining non-dimensional parameters. These equations are solved using a numerical technique namely Rung Kutta method resulting in bifurcation diagrams and Poincare´ portraits of the system. The system dynamical behavior for specific sets of system parameters is also plotted by means of phase plane portraits and Fast Fourier Transforms (FFTs). The main objective of the current study is to determine the effect of the axial speed and mass eccentricity on the string dynamical behavior.

2. EQUATIONS OF MOTION

Consider a uniform string of length l, which is travelling at a time dependent axial speed μ_p. The time dependent speed is assumed to vary harmonically about a mean axial speed. The string is assumed to be hinged at both ends. Shear deformation and rotary inertia are neglected that means the Euler Bernoulli beam model is used. The longitudinal and torsional vibrations are neglected in the model. In order to derive the equations of motion, extended Hamilton's principle is used [20]:

$$\delta\Pi = \int_{t_1}^{t_2} \delta(T - U + W_{nc})dt = 0 \tag{1}$$

where, δ denotes the variation, T is total kinetic energy of the system, U is potential energy and W_{nc} is the work done by non-conservative forces. Total kinetic energy of the system is:

$$T = \frac{1}{2}\int_0^l \left[\rho_p A_p \bar{V}^T \bar{V} + \rho_p \omega^T [I_t]\omega\right] dx \tag{2}$$

where, l is length of the string. A_p is cross sectional area. $\bar{V}$ is translational velocity vector of cross sectional area. ω and $[I_t]$ are angular velocity and the mass moment of inertia matrix per unit length of the string. v and w denote the two lateral deflections of point G relative to xyz reference frame (see Figure 1). μ_p is the string axial speed and considered as harmonic so that, $\mu_p = \mu_{p_0} + \mu_{p1}\sin(\omega_{\mu_p} t)$ [21, 22]. Where, μ_{p0} and μ_{p1} are constant and variable axial speed of the string, respectively. ω_{μ_p} is frequency of string variable axial speed. θ_x, θ_y and θ_z are rotation about x, y and z axis, respectively. Substituting $\bar{V}$, ω and $[I_t]$ in Equation (2) yields:

$$T = \frac{1}{2}\int_0^l \begin{bmatrix} \rho_p A_p \left(\left[\frac{\partial v}{\partial t} + \mu_p \frac{\partial v}{\partial x} - e(x)\frac{\partial \theta_x}{\partial t}\sin(\theta_x)\right]^2 \right. \\ \left. + \left[\frac{\partial w}{\partial t} + \mu_p \frac{\partial w}{\partial x} + e(x)\frac{\partial \theta_x}{\partial t}\cos(\theta_x)\right]^2\right) \\ + \rho_p I\left(\left(\frac{\partial^2 v}{\partial t \partial x}\right)^2 + \left(\frac{\partial^2 w}{\partial t \partial x}\right)^2\right) + \rho_p I_o \Omega^2 \\ -2\rho_p I_o \Omega \frac{\partial^2 v}{\partial t \partial x}\frac{\partial w}{\partial x} \end{bmatrix} \tag{3}$$

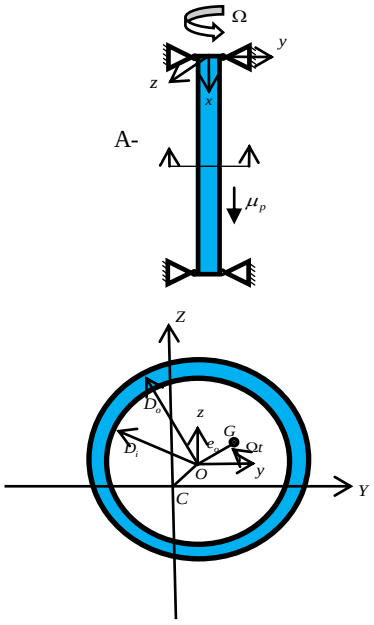

Figure 1. Cross sectional area of the axial moving string under rotation

If the mass eccentricity is assumed constant along the string, then $e(x)=e_0$ and the cross sectional area of the string is symmetric, $I=I_y=I_z$, $I_o=2I$ Where I_o is the moment of inertia about the string center line. By neglecting nonlinear terms (over order 2), the strain energy is written as:

$$U=\frac{1}{2}\int_0^l EI\left(\left(\frac{\partial^2 v}{\partial x^2}\right)^2+\left(\frac{\partial^2 w}{\partial x^2}\right)^2\right)dx \tag{4}$$

In which v and w are the displacements of lateral vibration in y and z directions, respectively and E is Young's modulus of the string. The virtual work due to lateral damping of the system can be written as [23]:

$$\delta W_{nc}=\int_0^l(-C_v\dot{v})\delta v dx+\int_0^l(-C_w\dot{w})\delta w dx \tag{5}$$

where, C_v and C_w are lateral damping coefficients of the string in v and w directions, respectively. Substituting Equations (3-5) in Equation (1) yields:

$$\begin{aligned}&\rho_p A_p\frac{\partial^2 v}{\partial t^2}+C_v\frac{\partial v}{\partial t}+\rho_p A_p\mu_p^2\frac{\partial^2 v}{\partial x^2}\\&+2\rho_p A_p\mu_p\frac{\partial^2 v}{\partial t\partial x}+\rho_p A_p\frac{\partial\mu_p}{\partial t}\frac{\partial v}{\partial x}+\rho_p I_o\Omega\frac{\partial^3 w}{\partial x^2\partial t}\\&-\rho_p I\frac{\partial^4 v}{\partial x^2\partial t^2}+EI\frac{\partial^4 v}{\partial x^4}-\rho_p A_p e_o\Omega^2\cos(\Omega t)=0\end{aligned} \tag{6}$$

$$\begin{aligned}&\rho_p A_p\frac{\partial^2 w}{\partial t^2}+C_w\frac{\partial w}{\partial t}+\rho_p A_p\mu_p^2\frac{\partial^2 w}{\partial x^2}\\&+2\rho_p A_p\mu_p\frac{\partial^2 w}{\partial t\partial x}+\rho_p A_p\frac{\partial\mu_p}{\partial t}\frac{\partial w}{\partial x}-\rho_p I_o\Omega\frac{\partial^3 v}{\partial x^2\partial t}\\&-\rho_p I\frac{\partial^4 w}{\partial x^2\partial t^2}+EI\frac{\partial^4 w}{\partial x^4}-\rho_p A_p e_o\Omega^2\sin(\Omega t)=0\end{aligned} \tag{7}$$

Where, Equations (6) and (7) are equations of motion of the string in transverse vibration in y and z directions, respectively. For a simply supported beam, the boundary conditions are:

$$\begin{aligned}&v(0,t)=v(l,t)=0,\frac{\partial^2 v(0,t)}{\partial x^2}=\frac{\partial^2 v(l,t)}{\partial x^2}=0\\&w(0,t)=w(l,t)=0,\frac{\partial^2 w(0,t)}{\partial x^2}=\frac{\partial^2 w(l,t)}{\partial x^2}=0\end{aligned} \tag{8}$$

Introducing next the following non-dimensional quantities:

$$\begin{aligned}&\tilde{t}=\sqrt{\frac{\rho_p A_p l^4}{EI}}\ e_0^*=\frac{e_0}{l}\ \tau=\frac{t}{\tilde{t}}\ \eta=\frac{v}{l}\ \zeta=\frac{w}{l}\ \hat{\omega}_{\mu_p}=\omega_{\mu_p}\tilde{t}\\&\hat{\Omega}=\Omega\tilde{t}\ \ \hat{C}_v=\frac{C_v l^2}{\sqrt{EI\,\rho_p A_p}}\ \ \hat{\mu}_p=\mu_p\sqrt{\frac{\rho_p A_p l^2}{EI}}\\&\hat{C}_w=\frac{C_w l^2}{\sqrt{EI\,\rho_p A_p}}\end{aligned} \tag{9}$$

Equations (6) and (7) can be written in a non-dimensional form as follows:

$$\begin{aligned}&\frac{\partial^2\eta}{\partial\tau^2}+\hat{C}_v\frac{\partial\eta}{\partial\tau}+\hat{\mu}_p^2\frac{\partial^2\eta}{\partial\xi^2}+2\hat{\mu}_p\frac{\partial^2\eta}{\partial\tau\partial\xi}+\frac{\partial\hat{\mu}_p}{\partial\tau}\frac{\partial\eta}{\partial\xi}\\&+\frac{I_o\hat{\Omega}}{A_p l^2}\frac{\partial^3\zeta}{\partial\xi^2\partial\tau}-\frac{I}{l^2A_p}\frac{\partial^4\eta}{\partial\xi^2\partial\tau^2}+\frac{\partial^4\eta}{\partial^4\xi}\\&-\frac{e_o\hat{\Omega}^2}{l}\cos(\hat{\Omega}\tau)=0\end{aligned} \tag{10}$$

$$\begin{aligned}&\frac{\partial^2\zeta}{\partial\tau^2}+\hat{C}_w\frac{\partial\zeta}{\partial\tau}+\hat{\mu}_p^2\frac{\partial^2\zeta}{\partial\xi^2}+2\hat{\mu}_p\frac{\partial^2\zeta}{\partial\tau\partial\xi}+\frac{\partial\hat{\mu}_p}{\partial\tau}\frac{\partial\zeta}{\partial\xi}\\&-\frac{I_o\hat{\Omega}}{A_p l^2}\frac{\partial^3\eta}{\partial\xi^2\partial\tau}-\frac{I}{l^2A_p}\frac{\partial^4\zeta}{\partial\xi^2\partial\tau^2}+\frac{\partial^4\zeta}{\partial^4\xi}\\&-\frac{e_o\hat{\Omega}^2}{l}\sin(\hat{\Omega}\tau)=0\end{aligned} \tag{11}$$

Non-dimensional equations are discretized by Galerkin's technique, with the simply supported beam eigen functions, $\psi_i(\xi)$, $\psi_j(\xi)$ being used as a suitable set of base functions and $q_i(\tau)$, $h_j(\tau)$ being the corresponding generalized coordinates. Thus:

$$\eta_i(\xi,\tau)=\sum_{i=1}^{N}\psi_i(\xi)q_i(\tau) \tag{12}$$

$$\zeta_j(\xi,\tau)=\sum_{j=1}^{M}\psi_j(\xi)h_j(\tau) \tag{13}$$

Substituting Equations (12) and (13) into Equations (10) and (11), respectively, multiplying by $\psi_n(\xi)$ and integrating with respect to x from 0 to 1, and then considering first mode yields:

$$\begin{aligned}&\ddot{q}_1\int_0^1\psi_1^2 d\xi+\dot{q}_1\hat{C}_v\int_0^1\psi_1^2 d\xi+\hat{\mu}_p{}^2 q_1\int_0^1\psi_1\psi_1'' d\xi\\&+2\hat{\mu}_p\dot{q}_1\int_0^1\psi_1\psi_1' d\xi+\frac{\partial\hat{\mu}_p}{\partial\tau}q_1\int_0^1\psi_1\psi_1' d\xi\\&+\frac{I_o\hat{\Omega}}{A_p l^2}\dot{h}_1\int_0^1\psi_1\psi_1'' d\xi-\frac{I}{A_p l^2}\ddot{q}_1\int_0^1\psi_1\psi_1'' d\xi\\&+q_1\int_0^1\psi_1\psi_1^{(4)} d\xi-\frac{e_o\hat{\Omega}^2}{l}\cos(\hat{\Omega}\tau)\int_0^1\psi_1 d\xi=0\end{aligned} \tag{14}$$

In which dot and prime notations stand for the differentiation with respect to non-dimensional time and axial coordinate, respectively. Simulation is based on a Rung Kutta technique order 15s in MATLAB software. Simulation parameters displayed in Table 1 represent a typical string for case study is taken from [16, 19].

$$\ddot{h}_1\int_0^1\psi_1^2 d\xi+\dot{h}_1\hat{C}_v\int_0^1\psi_1^2 d\xi+\hat{\mu}_p{}^2 h_1\int_0^1\psi_1\psi_1'' d\xi$$
$$+2\hat{\mu}_p\dot{h}_1\int_0^1\psi_1\psi_1' d\xi+\frac{\partial\hat{\mu}_p}{\partial\tau}h_1\int_0^1\psi_1\psi_1' d\xi$$
$$-\frac{I_o\hat{\Omega}}{A_p l^2}\dot{q}_1\int_0^1\psi_1\psi_1'' d\xi-\frac{I}{A_p l^2}\ddot{h}_1\int_0^1\psi_1\psi_1'' d\xi \quad (15)$$
$$+h_1\int_0^1\psi_1\psi_1^{(4)} d\xi-\frac{e_o\hat{\Omega}^2}{l}\sin(\hat{\Omega}\tau)\int_0^1\psi_1 d\xi=0$$

3. BIFURCATION DIAGRAMS AND POINCARE´ PORTRAITS

In this section, dynamical behavior of the system is examined numerically by means of Rung Kutta technique. In the calculations to construct the bifurcation diagrams, the transient solutions were discarded. At each set of parameters, the first 1900 points of the Poincare' portraits are discarded in order to exclude the transient vibration, and the generalized coordinates associated with displacement for the next 10 points are plotted on the bifurcation diagrams. Non-dimensional mean axial speed, non-dimensional fluctuating speed and mass eccentricity are considered as control parameters for plotting bifurcation diagrams, respectively.

3. 1. Non-dimensional Mean Axial Speed As Bifurcation Parameter Non-dimensional mean axial speed is considered as bifurcation parameter while the other parameters are fixed. Figure 2a shows the bifurcation diagram corresponding to the generalized coordinate q. Column of points are seen in each point of bifurcation parameter. Poincare' portraits are used for identifying quasi-periodic and chaotic motion. For the non-dimensional mean axial speed range of [0, 0.005] the system exhibits a quasi-periodic motion while the motion amplitude increases. Increasing the mean axial speed further, the amplitude of the motion increases and the system experiences a jump to higher amplitude at $\mu_{p0}^*=0.006$. By further incrementing the non-dimensional mean axial speed, the system exhibits increasing and then decreasing behavior in amplitude of motion repeatedly.

TABLE 1. Parameters of the string

$E=210GPa$	$\Omega=5rad/s$	$l=20m$
$D_o=0.22m$	$g=9.81m/s^2$	$\mu_p=0.1m/s$
$D_i=0.08m$	$\rho_p=7850kg/m^3$	$e^*{}_o=0.00025m$

In a full Poincare' portrait, quasi-periodic motion is represented by a closed curve while chaos is represented by an infinite number of points with a fine fractal structure. Poincare' portrait for non-dimensional mean axial speed in point $\mu_{p0}^*=0.001$ in Figure 2a is shown in Figure 3 for generalized coordinate q. As seen in the figure, the system response is reached closed curve after transient points that represents quasi-periodic motion. Track of the points are shown by red arrow in Poincare' portraits. Bifurcation diagram corresponding to the generalized coordinate h is shown Figure 2b. The system exhibits a quasi-periodic motion for non-dimensional mean axial speed range of [0, 0.016], while the motion amplitude doesn't increase significantly. As seen in Figure 2b, the motion amplitude of the system increases from $\mu_{p0}^*=0.016$ and then decreases. The motion amplitude at next increasing and decreasing state is larger than the previous. According to bifurcation diagram in Figure 2b, the system experiences jumps at $\mu_{p0}^*=0.032$ and $\mu_{p0}^*=0.034$.

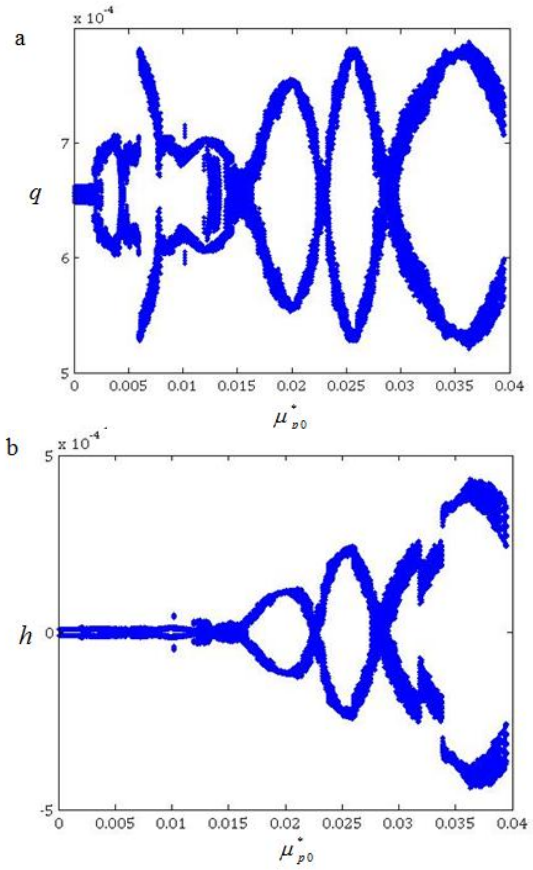

Figure 2. Bifurcation diagrams for non-dimensional mean axial speed for the system: (a) and (b) correspond to the q and h, respectively

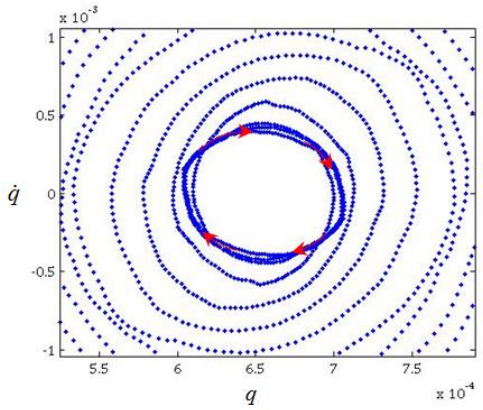

Figure 3. Poincare' portrait for non-dimensional mean axial speed at $\mu_{p0}^{*}=0.001$ in Figure 2a

3. 2. Non-dimensional Fluctuating Speed As Bifurcation Parameter Bifurcation diagrams for increasing non-dimensional fluctuating speed are shown in Figure 4. Non-dimensional fluctuating speed is considered as bifurcation parameter while the other parameters are fixed. Figure 4a shows the bifurcation diagram corresponding to the generalized coordinate q. For non-dimensional fluctuating speed range of [0, 0.01], the system response becomes quasi-periodic and stays almost the same until $\mu_{p1}^{*}=0.015$. The response decreases and stays almost the same in range of [0.022, 0.024]. By further incrementing the non-dimensional fluctuating speed, the system response amplitude increases and then decreases until it reaches to $\mu_{p1}^{*}=0.032$. By further increasing the fluctuation speed, the amplitude of the motion increases and then decreases. Poincare' portrait for fluctuation axial speed at point $\mu_{p1}^{*}=0.021$ for generalized coordinate q is shown in Figure 5. Response of the system is reached closed curve after transient points that indicates quasi-periodic motion. Figure 4b shows the bifurcation diagram corresponding to the generalized coordinate h. By incrementing the non-dimensional fluctuation speed, the system response stays almost the same until $\mu_{p1}^{*}=0.025$ .The system response increases and then decreases after point $\mu_{p1}^{*}=0.03$. This increasing and then deceasing behavior is repeated by further increasing the non-dimensional fluctuation speed. By increasing the non-dimensional fluctuation speed, the motion amplitude increases. Poincare' portrait for fluctuation axial speed at point $\mu_{p1}^{*}=0.001$ for generalized coordinate h is shown in Figure 6. The system response is reached closed curve after transient points that shows quasi-periodic motion.

3. 3. Mass Eccentricity As Bifurcation Parameter Figure 7 exhibits bifurcation diagram for generalized coordinate h with increasing mass eccentricity. As the mass eccentricity is increased, the amplitude of the motion increases accordingly.

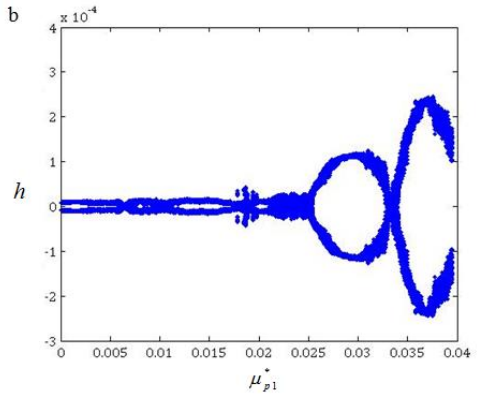

Figure 4. Bifurcation diagrams for non-dimensional fluctuation axial speed: (a) and (b) correspond to the q and h, respectively

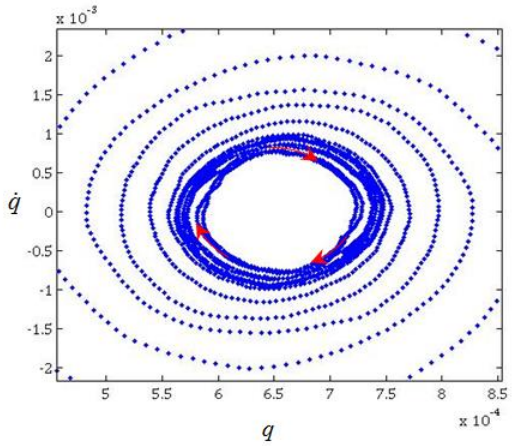

Figure 5. Poincare' portrait for fluctuation axial speed at $\mu_{p1}^{*}=0.021$ Figure 4a

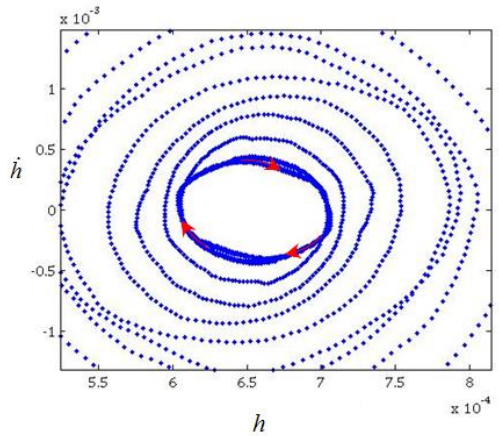

Figure 6. Poincare' portrait for fluctuation axial speed at $\mu_{p1}^{*}=0.001$ in Figure 4b

As the mass eccentricity is increased, the amplitude of the motion increases and then decreases. Poincare' portrait at point $e_o = 1.05e-4$ is shown in Figure 8. Dynamical behavior of the system is quasi-periodic. Also, by increasing the bifurcation parameter, the system response increases. The system hasn't jump in this case. In the second case, non-dimensional fluctuation speed was considered. Validation of the results is carried out by using phase plane portraits and Fast Fourier Transforms (FFTs). Phase plane portrait of the system for mean axial speed at $\mu_{p0}^{*} = 0.001$ is shown in Figure 9 that indicates quasi-periodic motion. FFT of Figure 9 is shown in Figure 10 and indicates quasi-periodic motion.

4. SUMMARY AND CONCLUSIONS

Bifurcation analysis of the rotational slender axially moving string is investigated. The coupled equations of motion were derived by means of Hamilton' principle.

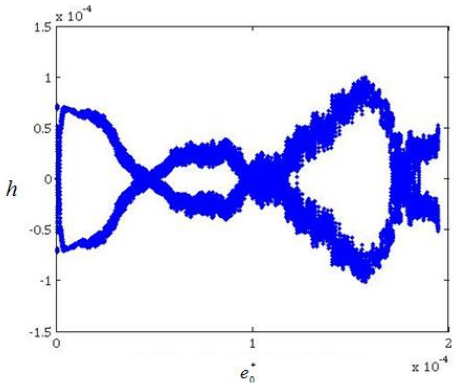

Figure 7. Bifurcation diagramof mass eccentricity for the generalized coordinate h

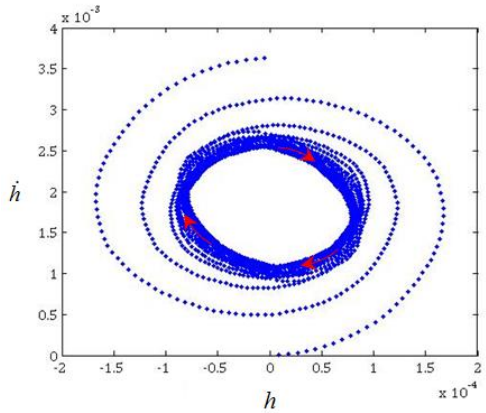

Figure 8. Poincare' portrait of mass eccentricity atpoint $e_o = 1.05e-4$ in Figure 7

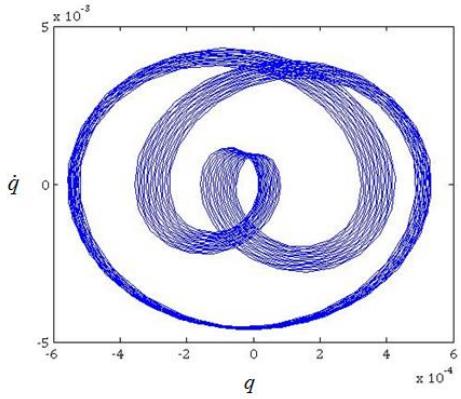

Figure 9. Phase-plane portrait of the system for mean axial speed at $\mu_{p0}^{*} = 0.001$ in Figure 3

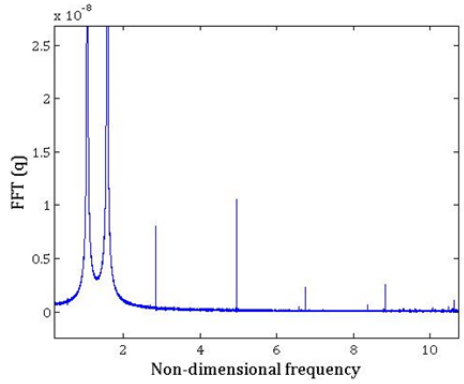

Figure 10. FFT of the system for mean axial speed as bifurcation parameter at $\mu_{p0}^{*} = 0.001$ in Figure 3

The Galerkin scheme was employed to transform the partial differential equations into ordinary differential equations. A number of variables were then introduced to these equations to transform them into non-dimensional form. The non-dimensional equations then solved numerically by means of Rung Kutta technique and bifurcation diagrams and Poincare' portraits were plotted. In the first case, non-dimensional axial speed was taken as the bifurcation parameter. Poincare' portraits indicated that the system is quasi-periodic motion in directions associated with v and w. The motion amplitude in displacement v is more than displacement w. Also, by increasing the bifurcation parameter the system response increases. The system experiences some jumps in this case. In the second case, non-dimensional fluctuation speed was considered as bifurcation parameter. Poincare' portraits indicated that the system shows quasi-periodic motion in each two directions. There isn't jump in this case. In the third case, mass eccentricity was taken as bifurcation parameter. Response amplitude of the system increases by increasing the mass eccentricity for generalized coordinate q. Poincare' portraits indicated that the

system is quasi-periodic motion in each two directions. There isn't jump in this case too. Poincare' portraits show quasi-periodic motion. The system behavior is different for two generalized coordinate q and h. Phase-plane portraits and FFTs are plotted to validate the diagrams. This research was carried out based on string middle rotational speed. Further studies can be done for different rotational speed using frequency response curve.

5. REFERENCES

1. Wicker, J. and Mote Jr, C., "Current research on the vibration and stability of axially-moving materials", ***The Shock and Vibration Digest***, Vol. 20, No. 5, (1988), 3-13.
2. Nayfeh, A.H. and Balachandran, B., Applied nonlinear dynamics: Analytical, computational, and experimental methods, in Wiley series in nonlinear sciences. (1995), John Wiley & Sons, Inc New York.
3. Argyris, J., Belubekian, V., Ovakimyan, N. and Minasyan, M., "Chaotic vibrations of a nonlinear viscoelastic beam", ***Chaos, Solitons & Fractals***, Vol. 7, No. 2, (1996), 151-163.
4. Pakdemirli, M. and Ulsoy, A., "Stability analysis of an axially accelerating string", ***Journal of Sound and Vibration***, Vol. 203, No. 5, (1997), 815-832.
5. Öz, H., Pakdemirli, M. and Boyacı, H., "Non-linear vibrations and stability of an axially moving beam with time-dependent velocity", ***International Journal of Non-Linear Mechanics***, Vol. 36, No. 1, (2001), 107-115.
6. Chen, L.-Q., Zhang, N.-H. and Zu, J.W., "Bifurcation and chaos of an axially moving viscoelastic string", ***Mechanics Research Communications***, Vol. 29, No. 2, (2002), 81-90.
7. Yang, X.-D. and Chen, L.-Q., "Bifurcation and chaos of an axially accelerating viscoelastic beam", ***Chaos, Solitons & Fractals***, Vol. 23, No. 1, (2005), 249-258.
8. Xiaodong ,Y. and Li-Qun, C., "Non-linear forced vibration of axially moving viscoelastic beams", ***Acta Mechanica Solida Sinica***, Vol. 19, No. 4, (2006), 365-373.
9. Modarres-Sadeghi, Y., "Nonlinear dynamics of a slender flexible cylinder subjected to axial flow, Vol. 68, (2006).
10. Pan, L., Qiao, N., Lin, W. and Liang, Y., "Stability and local bifurcation in a simply-supported beam carrying a moving mass", ***Acta Mechanica Solida Sinica***, Vol. 20, No. 2, (2007), 123-129.
11. Korayem, M. and Alipour, A., "Dynamic analysis of moving cables with variable tension and variable speed", (2010).
12. Ding, H. and Chen, L.-Q., "Nonlinear models for transverse forced vibration of axially moving viscoelastic beams", ***Shock and Vibration***, Vol. 18, No. 1-2, (2011), 287-281.
13. Ghayesh, M.H., Amabili, M. and Farokhi, H., "Coupled global dynamics of an axially moving viscoelastic beam", ***International Journal of Non-Linear Mechanics***, Vol. 51, (2013), 54-74.
14. Hosseini, S., Zamanian, M., Shams, S. and Shooshtari, A., "Vibration analysis of geometrically nonlinear spinning beams", ***Mechanism and Machine Theory***, Vol. 78, (2014), 15-35.
15. Shahgholi, M., Khadem, S. and Bab, S., "Free vibration analysis of a nonlinear slender rotating shaft with simply support conditions", ***Mechanism and Machine Theory***, Vol. 82, (2014), 128-140.
16. Sahoo, B., Panda, L. and Pohit, G., Stability and bifurcation analysis of an axially accelerating beam, in Vibration engineering and technology of machinery. 2015, 915-928.
17. Dykstra, M.W., "Nonlinear drill string dynamics, Graduate School, (1996).
18. Van Der Heijden, G.H., "Bifurcation and chaos in drillstring dynamics", ***Chaos, Solitons & Fractals***, Vol. 3, No. 2, (1993), 219-247.
19. Shyu, R.-J., "Bending vibration of rotating drill strings", Massachusetts Institute of Technology, (1989)
20. Sahebkar, S., Ghazavi, M., Khadem, S. and Ghayesh, M., "Nonlinear vibration analysis of an axially moving drillstring system with time dependent axial load and axial velocity in inclined well", ***Mechanism and Machine Theory***, Vol. 46, No. 5, (2011), 743-760.
21. Meirovitch, L., "Analytical methods in vibrations, 1967", ***McMillan, New York***.
22. Lesieutre, G.A., "Frequency-independent modal damping for flexural structures via a viscous" geometric" damping model", ***Journal of guidance, control, and dynamics***, Vol. 33, No. 6, (2010), 1931-1935.
23. Oz, H., "On the vibrations of an axially travelling beam on fixed supports with variable velocity", ***Journal of Sound andVibration***, Vol. 239, No. 3, (2001), 556-564.

Nonlinear Dynamics of the Rotational Slender Axially Moving String with Simply Supported Conditions

H. Heydari[a], M.R. Ghazavi[a], A. Najafi[b], S. Rahmanian[a]

[a] *Department of Mechanical Engineering, Tarbiat Modares University, Tehran, Iran*
[b] *Mechanical Rotary Equipment Department, Niroo Research Institute, Tehran, Iran*

P A P E R I N F O

Paper history:
Received 16 December 2015
Received in revised form 07 April 2016
Accepted 02 June 2016

Keywords:
String
Axial Speed
Bifurcation Diagram
Poincare Portrait
Quasi-periodic

چکیده

در این تحقیق، آنالیز دینامیکی رشته دارای حرکت محوری و چرخشی بررسی می‌شود. رشته به صورت تیر اویلر برنولی فرض می‌شود.حرکت محوری رشته، نیروی ژیروسکوپی و خروج از مرکزیت جرم در این مطالعه در نظر گرفته شده‌اند.معادلات حرکت با استفاده از اصل همیلتون استخراج شده و دو معادله دیفرانسیل برای حرکت عرضی بدست می‌آید.معادلات حرکت به شکل بی‌بعد تبدیل شده و با استفاده از روش گالرکین گسسته‌سازی می‌شوند. نمودارهای انشعاب و نگاشت‌های پوانکاره در حالتی که سرعت محوری میانگین، سرعت محوری نوسانی و خروج از مرکزیت جرم تغییر می‌کنند، بدست می‌آیند. رفتارهای دینامیکی بر اساس نگاشت‌های پوانکاره تعیین می‌شوند. شبیه‌سازی‌های عددی، با تغییر سرعت محوری و خروج از مرکزیت جرم، حرکت شبه‌پریودیک را در ارتعاشات عرضی نشان می‌دهند.

***doi**: 10.5829/idosi.ije.2016.29.06c.13*